



Commentary

X-ray structure breakthroughs in the GPCR transmembrane region

Sid Topiol*, Michael Sabio

Department of Computational Chemistry, Lundbeck Research USA, Inc., 215 College Road, Paramus, NJ 07652, USA

ARTICLE INFO

Article history:

Received 21 January 2009

Accepted 16 February 2009

Keywords:

GPCR

X-ray structures

Rhodopsin

 β_1 -Adrenergic receptor β_2 -Adrenergic receptor A_{2A} adenosine receptor

ABSTRACT

G-protein-coupled receptor (GPCR) proteins [Lundstrom KH, Chiu ML, editors. G protein-coupled receptors in drug discovery. CRC Press; 2006] are the single largest drug target, representing 25–50% of marketed drugs [Overington JP, Al-Lazikani B, Hopkins AL. How many drug targets are there? *Nat Rev Drug Discov* 2006;5(12):993–6; Parrill AL. Crystal structures of a second G protein-coupled receptor: triumphs and implications. *ChemMedChem* 2008;3:1021–3]. While there are six subclasses of GPCR proteins, the hallmark of all GPCR proteins is the transmembrane-spanning region. The general architecture of this transmembrane (TM) region has been known for some time to contain seven α -helices. From a drug discovery and design perspective, structural information of the GPCRs has been sought as a tool for structure-based drug design. The advances in the past decade of technologies for structure-based design have proven to be useful in a number of areas. Invoking these approaches for GPCR targets has remained challenging. Until recently, the most closely related structures available for GPCR modeling have been those of bovine rhodopsin. While a representative of class A GPCRs, bovine rhodopsin is not a ligand-activated GPCR and is fairly distant in sequence homology to other class A GPCRs. Thus, there is a variable degree of uncertainty in the use of the rhodopsin X-ray structure as a template for homology modeling of other GPCR targets. Recent publications of X-ray structures of class A GPCRs now offer the opportunity to better understand the molecular mechanism of action at the atomic level, to deploy X-ray structures directly for their use in structure-based design, and to provide more promising templates for many other ligand-mediated GPCRs. We summarize herein some of the recent findings in this area and provide an initial perspective of the emerging opportunities, possible limitations, and remaining questions. Other aspects of the recent X-ray structures are described by Weis and Kobilka [Weis WI, Kobilka BK. Structural insights into G-protein-coupled receptor activation. *Curr Opin Struct Biol* 2008;18:734–40] and Mustafi and Palczewski [Mustafi D, Palczewski K. Topology of class A G protein-coupled receptors: insights gained from crystal structures of rhodopsins, adrenergic and adenosine receptors. *Mol Pharmacol* 2009;75:1–12].

© 2009 Elsevier Inc. All rights reserved.

1. Introduction

The advantage of drug design with the aid of the target protein's three-dimensional structure has now been well established. It is not surprising that the interest in applying such structure-based design methods to G-protein-coupled receptor (GPCR) targets [1], the largest single drug target class [2,3] has been sought for quite some time. In particular, the structure of the common denominator of GPCRs, i.e., the transmembrane (TM) region, has been the ultimate goal. Towards this end, there has been a continual progression of advances bringing this goal closer to realization. Starting in 2000, the first high-resolution X-ray structures of GPCRs, those of bovine

rhodopsin, began to emerge (see Table 1 and references cited therein). Rhodopsin is a light- (vs. ligand-) activated class A GPCR. Most of the bovine rhodopsin structures contain the covalently bound endogenous chromophore retinal in the “dark” (inactive) state [4,5]. An important feature of bovine rhodopsin that rendered it considerably more accessible to structure determination was its availability in relative high concentrations compared to other GPCRs. Studies following these results began to demonstrate that significant insights, e.g., into the role of water molecules in the mechanism of rhodopsin activation, were facilitated [6]. However, it soon became clear (e.g., see Refs. [7–9]) that even for class A GPCRs, the use of the bovine rhodopsin X-ray structures as templates for ligand-mediated GPCRs was a challenging and generally arduous undertaking with limited accuracy as a drug discovery tool, compared with the direct use of X-ray structures or homology models from closely related proteins in other target classes.

* Corresponding author. Tel.: +1 201 350 0389; fax: +1 201 261 0623.

Table 1
X-ray diffraction class A GPCR structures released by the PDB.

Accession ID	Resolution (Å)	Release date	Protein and active-site occupancy	Literature reference
A. (Rhod)opsin				
1F88	2.8	2000.08.04	Bovine rhodopsin with retinal	[66]
1HZX	2.8	2001.07.04	Bovine rhodopsin with retinal	[67]
1L9H	2.6	2002.05.15	Bovine rhodopsin with retinal	[6]
1GZM	2.65	2003.11.20	Bovine rhodopsin with retinal	[68]
1U19	2.2	2004.10.12	Bovine rhodopsin with retinal	[69]
2HPY	2.8	2006.08.22	Bovine lumirhodopsin with retinal	[70]
2G87	2.6	2006.09.02	Bovine bathorhodopsin with retinal	[71]
2I35	3.8	2006.10.17	Bovine rhodopsin with retinal	[72]
2I36	4.1	2006.10.17	Bovine rhodopsin with retinal ^a	[72]
2I37	4.15	2006.10.17	Bovine rhodopsin with retinal ^a	[72]
2J4Y	3.4	2007.09.25	Bovine rhodopsin with retinal	[73]
2PED	2.95	2007.10.30	Bovine rhodopsin with 9- <i>cis</i> -retinal	[74]
2ZIY	3.7	2008.05.06	Squid rhodopsin with retinal	[57]
2Z73	2.5	2008.05.13	Squid rhodopsin with retinal	[58]
3CAP	2.9	2008.06.24	Bovine opsin, ligand-free rhodopsin	[59]
3C9L	2.65	2008.08.05	Bovine rhodopsin with retinal	[75]
3C9M	3.4	2008.08.05	Bovine rhodopsin with retinal	[75]
3DQB	3.2	2008.09.23	Bovine opsin, ligand-free rhodopsin	[60]
B. Other Class A GPCRs				
2RH1	2.4	2007.10.30	Human β_2 -adrenergic receptor with carazolol	[30]
2R4R	3.4	2007.11.06	Human β_2 -adrenergic receptor with carazolol ^a	[29]
2R4S	3.4	2007.11.06	Human β_2 -adrenergic receptor with carazolol ^a	[29]
3D4S	2.8	2008.06.17	Human β_2 -adrenergic receptor with timolol	[45]
2VT4	2.7	2008.06.24	Turkey β_1 -adrenergic receptor with cyanopindolol	[56]
3EML	2.6	2008.10.14	Human A_{2A} adenosine receptor with ZM241385	[51]

^a The resolution in the active site was insufficient to determine the chromophore's or ligand's coordinates.

A number of limitations, questions, and challenges thus remained following the availability of the above bovine rhodopsin structures. Perhaps, foremost was the question of whether other GPCRs that do not have the relatively high natural abundance of bovine rhodopsin could be made amenable to X-ray structure determination. Indeed, for 7 years, bovine rhodopsin remained the only GPCR for which X-ray structures were available. One expectation, to be tested, was whether the availability of a high-resolution X-ray structure of a ligand-mediated GPCR would be as useful for structure-based design as has been observed for other protein classes, such as kinases and proteases. Furthermore, would such a template offer a useful starting point for homology modeling of related GPCRs? Would there be significant differences in GPCR structures within and between classes? Would it become possible to have reliable models for other states of GPCRs? Specifically, the initial bovine rhodopsin structures correspond to the inactive state. It is widely believed that GPCR proteins exist in multiple states, and information, e.g., on an active state, would be expected to have profound impact on structure-based design of agonists. Finally, would it be possible to understand the molecular mechanisms of GPCR activation and G-protein coupling? In this article, we summarize the impact of a series of recently published X-ray structures that open the door to address many of these questions as well as early studies that provide initial glimpses of the answers.

2. The pre-bovine rhodopsin era: before 2000

The overall topology of the transmembrane region of bacteriorhodopsin was determined to be comprised of 7 α -helices [10,11]. Electron cryo-microscopy results [12] showed that the bovine rhodopsin structure also has a 7-TM α -helical configuration. While the arrangement of the transmembrane helices was different, the determination of the X-ray structure of bacteriorhodopsin at low resolution [13] followed by the higher resolution [14] bacteriorhodopsin structure precipitated studies using these as templates upon which to model GPCRs of interest for drug design [9,15]. Structure–activity relationships, site-directed muta-

genesis data, and affinity-labeling efforts have been utilized to refine the bacteriorhodopsin-based models. For example, Underwood et al. docked [16] the non-peptide type-1 angiotensin II (AT_1) antagonist losartan into a bacteriorhodopsin-based homology model of the AT_1 receptor, such that the binding pose was consistent with known mutagenesis data. Other examples have been reviewed [17–21] in the literature. Unfortunately, in addition to the fact that bacteriorhodopsin is not a G-protein-coupled receptor, its distant relation to GPCRs of interest renders it difficult to be used as a template.

3. The bovine rhodopsin era: 2000–2007

In June 2000, the first X-ray diffraction structure of a GPCR, namely bovine rhodopsin at 2.8 Å resolution, was deposited in the Protein Data Bank (PDB ID = 1F88). At the end of that year, the PDB collection contained 16,363 X-ray entries, of which only 602 represented integral-membrane proteins including the one example of bovine rhodopsin. Since then, an additional 17 (bovine and squid) rhodopsin X-ray structures were deposited in the PDB, as enumerated in Table 1. The X-ray structures of bovine rhodopsin and bacteriorhodopsin are significantly different [19] including the positions, orientations, and packing of the α -helices [18,22,23]. In addition, a suitable superimposition of these two receptors cannot be achieved due to the α -helix kinks in bovine rhodopsin and the more regularly shaped α -helices in bacteriorhodopsin. The geometric differences and the greater sequence homology of bovine rhodopsin to GPCR targets of interest were expected to provide a major advantage in the use of bovine rhodopsin-based homology models.

The 18 (bovine and squid) rhodopsin X-ray structures including (when present) the covalently bound chromophore, retinal, are quite superimposable, especially in the transmembrane region. Retinal is tightly enclosed in a mainly lipophilic binding pocket (see Figs. 1 and 2). At one end, 11-*cis* retinal, the chromophore, covalently binds to Lys296. At the other end, the β -ionone ring is buried in a hydrophobic pocket formed by Trp265, Phe212, and Tyr268. The interaction between the β -ionone ring and Trp265

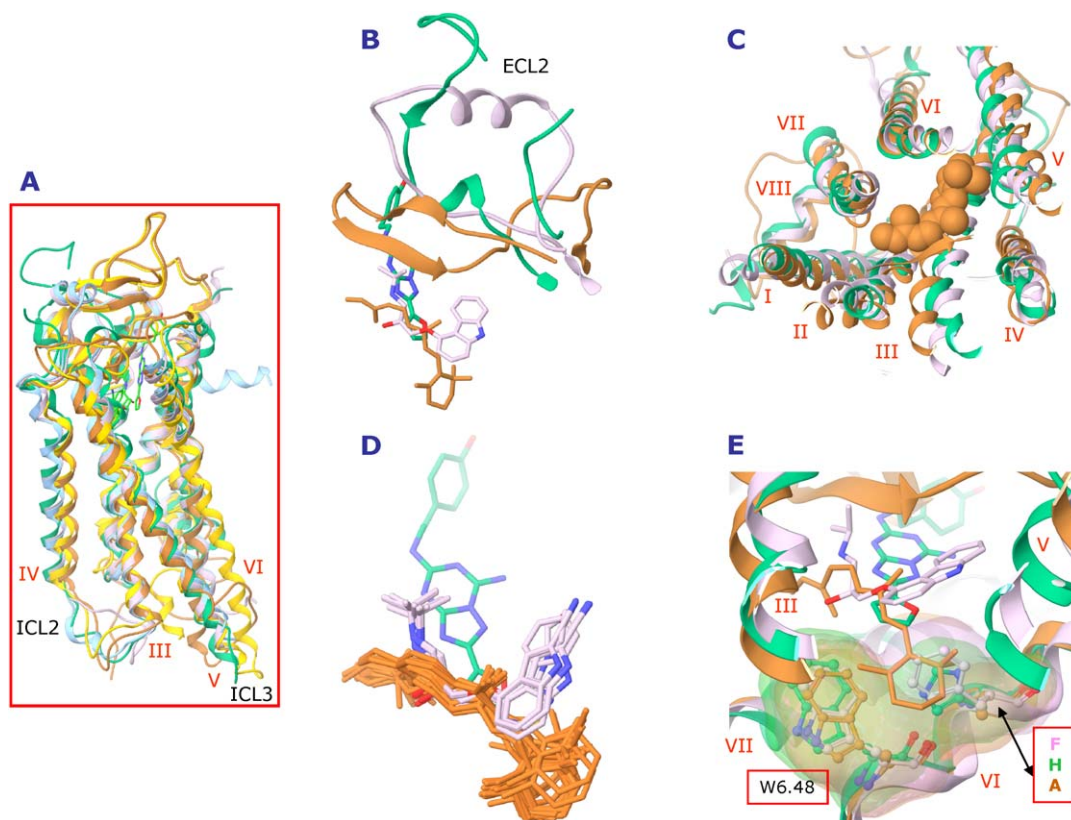


Fig. 1. Various noteworthy binding site, structural, and activation features are represented by four selected GPCR structures (1U19, bovine rhodopsin in brown; 2RH1, human β_2 -adrenergic receptor in pink; 2VT4, turkey β_1 -adrenergic receptor in aqua; 3DQB, bovine opsin in yellow; and 3EML, human A_{2A} adenosine receptor in green). Stabilizing companion proteins (e.g., T4L) are not shown in any of this figure's panels, and only chain A is used whenever a protein is displayed; (A) an overlay of the entire protein and ligand/chromophore of each selected GPCR structure; (B) the ECL2 region of bovine rhodopsin with retinal; the human β_2 -adrenergic receptor with carazolol; and the human A_{2A} adenosine receptor with ZM241385; (C) with truncation of the EC loop region for visual clarity, retinal is shown within the binding site of bovine rhodopsin, which is superimposed with the human β_2 -adrenergic receptor and the human A_{2A} adenosine receptor; (D) superimposition of all PDB chains of all GPCR proteins featured in Table 1 to show the relative positions of the chromophores and ligands and to show the variation in coordinates for multiple occurrences of the same chromophore or ligand; for visual clarity no protein is shown; (E) superimposition of bovine rhodopsin with retinal; the human β_2 -adrenergic receptor with carazolol; and the human A_{2A} adenosine receptor with ZM241385 in the "toggle switch" region viewed from inside the core towards the EC side. Note that the residues corresponding to Phe290 in the human β_2 -adrenergic receptor are Ala in rhodopsin and His in the A_{2A} adenosine receptor. All figure components were created in Maestro (Schrödinger [76]).

forces the side-chain rotamer conformation of Trp265 to be that of the inactive state. Switching between this and the active Trp265 conformation initiates the so-called "toggle switch" for activation/inactivation of rhodopsin.

The issues limiting the usefulness of bovine rhodopsin as an X-ray template for homology model construction of other GPCR proteins include (a) the uncertainty in aligning [20] GPCR sequences of interest, e.g., for loop regions or class B and C GPCRs, with that of bovine rhodopsin, which shares only a low level of overall sequence identity of perhaps 20% or less (and lower in the loop regions); an alignment error of even a single residue could render the resulting model unusable for drug design; (b) the questionable reliance on a GPCR X-ray template that covalently binds its ligand/chromophore; (c) the uncertainty of whether other GPCR proteins would adopt the same binding-site geometry, with respect to the disposition and bending of α -helices and the rotational states of the residues, of this single example of an inactive-state GPCR X-ray structure; (d) the necessary expansion from a tight binding cavity into a homology model, which is a consequence of the cramped bovine rhodopsin's geometry, to accommodate GPCR ligands of varying sizes; (e) the blocking of the bovine rhodopsin binding site by the E2 loop, which folds into the receptor to help completely enclose retinal with no obvious entry or exit pathway for ligands; and (f) the decision to model a GPCR target as a monomer, homodimer, heterodimer, or oligomer. The practice of using a single conformation of a GPCR homology model

(typically based on the inactive-state bovine rhodopsin X-ray structure) to analyze agonists, antagonists, and inverse agonists can be confounding, because a GPCR target exists in multiple conformations that depend on the nature and function of the target's ligands [20]; multiple conformations may exist even for the active state. With only inactive-state GPCR X-ray structures available and because the conformational changes resulting from GPCR activation are difficult to predict, the construction of an active-state homology model is very arduous and often begins by attempts to expand the binding site and rearrange (translate and rotate) the 7-TM α -helices.

Despite the uncertainties and difficulties in constructing bovine-rhodopsin-based GPCR homology models, successful outcomes in the use of such homology models have been reported (see, e.g., a recent review [9]). For example, Bissantz et al. constructed [8] homology models of the antagonist-bound form of three human GPCRs (dopamine D3, muscarinic M1, and vasopressin V1a) and the "agonist-bound" form of three human GPCRs (dopamine D3, β_2 -adrenergic, and δ -opioid) using the PDB's 1F88 X-ray structure of bovine rhodopsin as a structural template. After screening six 3D databases (each comprised of 990 random analogues plus 10 known antagonists or agonists for each target) with three docking algorithms using seven scoring functions, the authors concluded that bovine-rhodopsin-based homology models were effective in retrieving known antagonists that were seeded in the database but were not sufficiently accurate for identifying

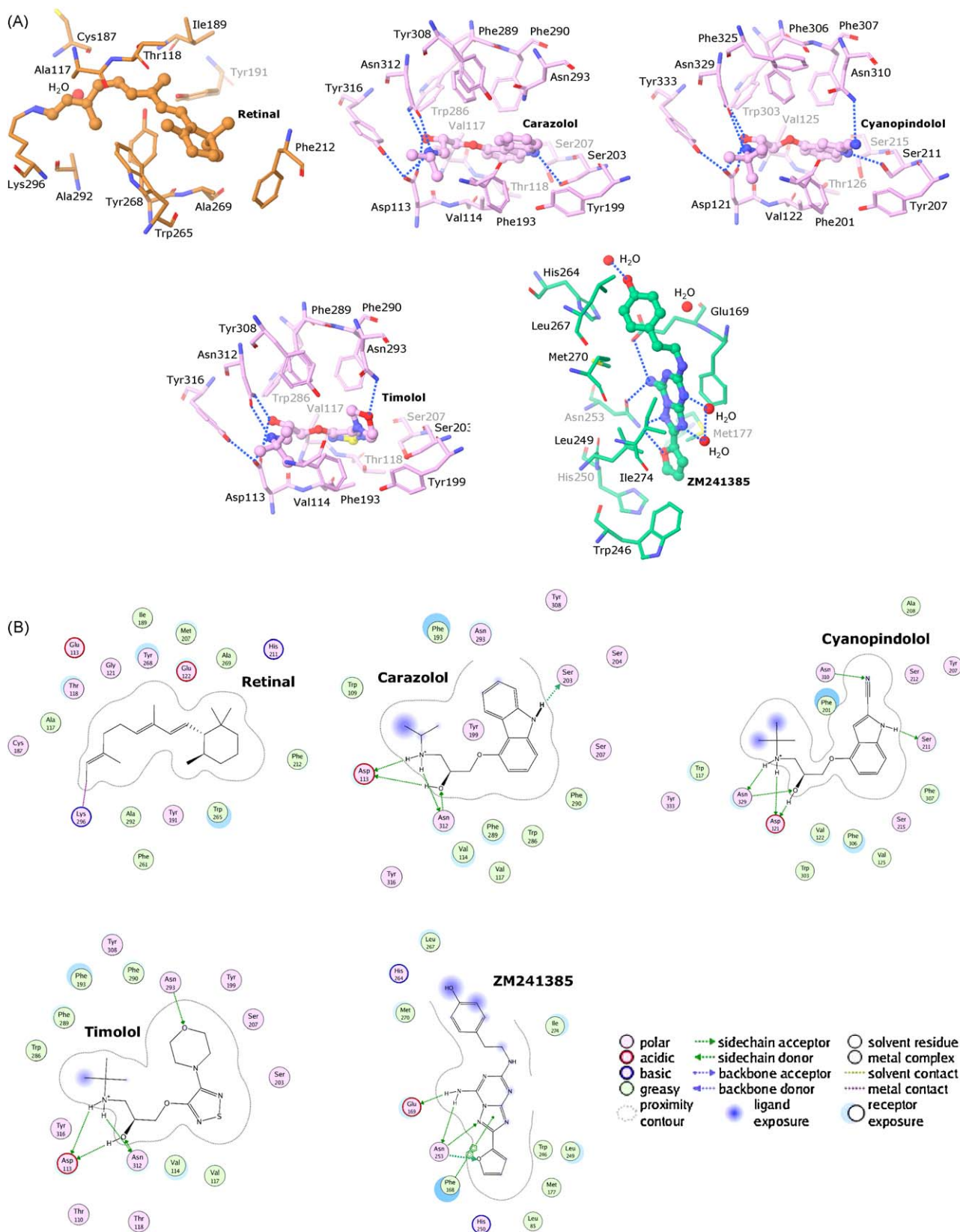


Fig. 2. (A) X-ray binding sites of bovine rhodopsin with retinal (1U19); the human β_2 -adrenergic receptor with carazolol (2RH1); the turkey β_1 -adrenergic receptor with cyanopindolol (2VT4); the human β_2 -adrenergic receptor with timolol (3D4S); and the human A_{2A} adenosine receptor with ZM241385 (3EML); (B) 2D-interaction maps for the X-ray complexes of this figure's part A. Three of the 2D maps were modified by addition of graphical components so that the maps would be compatible with the binding site depictions: a hydrogen bond between Ser203 and carazolol's carbazole NH unit was added; a hydrogen bond between Tyr316 and timolol's ammonium group was erased; and a hydrogen bond between Asn253 and ZM241385's furan oxygen atom was added. The 3D binding site depictions and (modified, as described above), 2D-interaction maps were created in Maestro (Schrödinger [76]) and MOE (Chemical Computing Group [77]), respectively.

known agonists. For the development of agonist models, the authors also invoked a knowledge- and pharmacophore-based modeling protocol that they developed. Heavy reliance on experimental results (e.g., mutational data, SAR, etc.) has been a key to successful construction and validation of models [9]. For example, Xie et al. developed [24] a bovine-rhodopsin-based homology model of the human CB₂ receptor, which agreed well with known biochemical and structural data. By using *ab initio* structure prediction algorithms, MembStruk and HierDock, Vaidehi et al. reproduced [25] the X-ray crystal structure of bovine rhodopsin to within an RMS difference of 3.1 Å inside the transmembrane region. For four classes of GPCR targets (β₁AR, EDG6, the human sweet receptor, and mouse/rat I7 olfactory receptors), the authors predicted protein structure and function in the absence of experimental structures. Attempts at avoiding the use of bovine rhodopsin as a template have also been described. Combining knowledge of the amino acid sequence with properties of the membrane environment, Shacham et al. developed [26] an algorithm, PREDICT, which does not utilize information derived from the rhodopsin 3D structure. The methodology reproduced the rhodopsin X-ray geometry within an RMS difference of 3.87 Å inside the transmembrane region and showed promise in generating other GPCR homology models for structure-based drug discovery, including the screening of virtual libraries. To help compensate for the limitations of the bovine rhodopsin X-ray structure as a template for GPCR homology model construction, various ligand-based approaches coupled with the use of structure–activity relationships, site-directed mutagenesis data, and affinity-labeling studies have been integrated to enhance the success of homology modeling [23]. Such hybrid approaches include the use of receptor–ligand pharmacophores [27] and ligand-based homology modeling [28]. Moreover, while there have been some encouraging examples [18–21], they are limited, and the paucity of high-resolution X-ray structures has prevented structure-based design from reaching the stage of a front-line production tool for GPCR drug design.

4. The GPCR X-ray structure parade of 2007–2008

4.1. The β₂-adrenergic receptor/carazolol complex: the first ligand-mediated GPCR to be crystallized

The bovine rhodopsin X-ray structures were the first true GPCR X-ray structures and represented a monumental step in this field. It provided a window into the atomic detail of the architecture of a GPCR and a structural framework for understanding a vast amount of experimental data on GPCR function. Generally speaking, for a given protein class, the first specific structure obtained yields the greatest single advancement in the information provided. Following this initial, single picture, the X-ray structure of the second protein in a class will also have significant impact as it starts to thaw out the frozen picture of the proteins in the given class. It provides the first opportunity to examine changes in the structure and possible consequences. The X-ray structures of the β₂-adrenoreceptor (PDB accession IDs 2R4R, 2R4S, and 2RH1) complexed with the picomolar affinity inverse agonist carazolol (2RH1) were the first GPCR structures published [29–31] since those of bovine rhodopsin. Whether these X-ray structures are characterized as the “second” GPCR structures or the “first” ligand-mediated GPCR structures, it was immediately obvious that they represented a breakthrough that is living up to expectations. These X-ray structure determinations used two different approaches. A number of techniques, including ligand–affinity chromatography, embedding in a lipid cubic phase, and stabilization were employed [32–34]. In both efforts, a key ingredient was that the flexible intracellular loop 3 (IL3) was stabilized by the use of a companion

protein. In the first work, a monoclonal antibody binding to this loop was obtained and used to form a complex that helped stabilize the two very similar proteins (one had the addition of a TEV cleavage site after amino acid 24 of the N-terminus) and facilitate crystallization. This resulted in two 3.4 Å-resolution structures in which the active site was poorly resolved [29]. In the second work, a portion of the ICL3 loop was excised and replaced with T4 Lysozyme (T4L). The T4L insertion also helped stabilize and crystallize the protein and resulted in a 2.4 Å-resolution structure complexed to carazolol. The mere solution of these structures provided the answer to the questions of if and when X-ray structures of GPCRs other than rhodopsin could be obtained. In fact, two different methods were proven possible. While providing no guarantees as to how quickly or easily the approaches could be extended to other targets, unlike the case of rhodopsin, there was nothing intrinsically specific to β₂AR to suggest such limitations (indeed, see below). The high-resolution β₂AR structure (to which we refer henceforth as the “β₂AR structure,” unless indicated otherwise) provided new as well as surprising information which answered some questions and raised others.

While the overall architecture of the β₂-adrenergic receptor resembles that of rhodopsin, there are changes in the tertiary structure and the positions of helices I, III, IV, V, and VI [29–31] (see Figs. 1 and 3). Whereas the much longer second extracellular loop of rhodopsin has a β-sheet structure that drapes over the active site, the ECL2 region of β₂AR is very different (see panels A and B of Fig. 1). An unexpected α-helix that has two cysteine bridges was found in ECL2. One of these bridges is within the ECL2 and the other is linked to transmembrane helix 3. These features hold ECL2 further from the core of the transmembrane region, providing more accessible ligand entry and, consequently, addressing the same question raised in relation to the ECL2-capped active site in the X-ray structure of bovine rhodopsin. The conformation of ECL2 provides an open architecture for facile ligand entry into the active site which contrasts with blockage of the extracellular side of the active site by ECL2 in the above described rhodopsin X-ray structure. The overall binding pocket in the β₂AR is more open than in rhodopsin.

The location and general topology of carazolol, the bound ligand, overlaps with the corresponding location of retinal in rhodopsin (see Fig. 1). Whereas retinal is covalently bound to rhodopsin, carazolol is anchored at one end by two polar residues, Asn312 and Asp113, each of which forms hydrogen bonds with both the hydroxy and amino portions of the hydroxy alkylamine side-chain (see Fig. 2). The hydrophobic carbazole ring of carazolol is buried in a hydrophobic pocket formed by residues Phe289, Phe290, Trp286, and Phe193. In addition, Ser203 is close to the carbazole nitrogen atom of carazolol. Trp286 corresponds to Trp265 of the “toggle switch” in rhodopsin. The rotameric conformation of Trp286 also corresponds to the inactive state, but is achieved by indirect interaction of the ligand with Phe289 and Phe290, which, in turn, hold Trp286 in the inactive conformation. Interestingly, Phe193, which also forms a hydrophobic interaction with the carbazole portion of carazolol, resides on ECL2. This level of detail of the interactions between residues on ECL2 with the ligand underscores the need for X-ray structure determinations of this highly variable region.

Some, but not all, of the hypotheses for GPCR activation have found support in these first structures. In the rhodopsin structure, immediately below the covalently bound retinal (and towards the intracellular side), there is a conserved tryptophan residue (W6.48, using established nomenclature [35]; see panel E of Fig. 1). This tryptophan is part of a series of side-chain residues that interact along the inner transmembrane region connecting to the intracellular side and, together with a network of conserved water molecules, propagate the activation/inactivation signal.

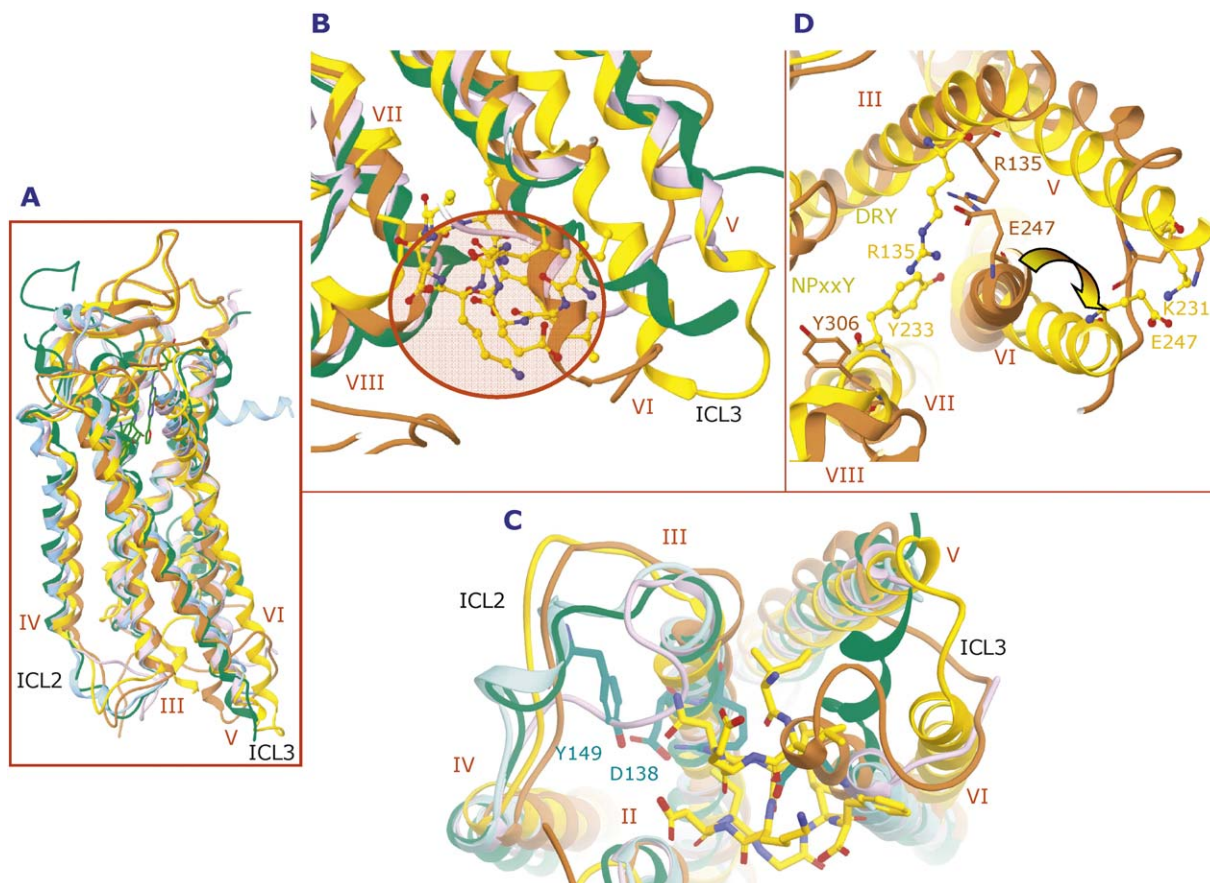


Fig. 3. (A) an overlay of the entire protein and ligand/chromophore of each selected GPCR structure named in Fig. 1; (B) side view of the superimposition of bovine rhodopsin; bovine opsin with bound G α CT; the human β_2 -adrenergic receptor; and the human A $_{2A}$ adenosine receptor; (C) view from the IC side into the core of a superimposition of bovine rhodopsin; bovine opsin with G α CT; the human β_2 -adrenergic receptor; the human β_1 -adrenergic receptor (showing selected residues); and the human A $_{2A}$ adenosine receptor; (D) view from the IC side into the core of a superimposition of bovine rhodopsin and bovine opsin with G α CT; selected residues involved in the “ionic lock” are displayed. All figure components were created in Maestro (Schrödinger [76]). The color scheme is the same as that used in Fig. 1.

W6.48 is believed to be the “toggle switch” for this signal as controlled by its rotational state. In rhodopsin, retinal sits deeply in the pocket (see panels C and D of Fig. 1) and its β -ionone ring interacts directly with W6.48, locking it into its inactive conformation (see panel E of Fig. 1). The binding of carazolol in the β_2 AR structure is not sufficiently deep to interact directly with W6.48, but instead, carazolol recruits Phe290 (whose corresponding residue is alanine in rhodopsin) as an intermediary, forcing the same (inactivating) conformation of W.68 (see panel E of Fig. 1). This consistency between the structures of inactive rhodopsin and β_2 AR is not as clear in the structures of the “ionic lock” region. The inverse agonist nature of carazolol for the native protein and its preserved affinity for the β_2 AR-T4L construct would suggest inactive characteristics for this construct. Using fluorescent probes, the authors showed that agonists can induce protein conformational changes consistent with receptor activation [31]. In the β_2 AR structure, residues D130^{3.49}, R131^{3.50}, and Y132^{3.51} form the (“D(E)RY”) motif involved with E247^{6.30} in the so-called “ionic lock,” which had been understood to characterize the inactive state and is supported by biophysical data [36,37]. Nevertheless, both the antibody-complexed and T4L-spliced X-ray structures of β_2 AR lack the “ionic lock.” This raised new questions. Is the absence of the “ionic lock” in these structures an artifact of the utilized methods that introduced large proteins (antibody, T4L) into the crystal structures? Is the “ionic lock” hypothesis incorrect? Does the inverse agonist (vs. antagonist) nature of the ligand, carazolol, induce a protein conformation that is different from that of the inactive state as evidenced by its basal activity? Indeed, consider-

able evidence has been presented to show that β_2 AR has multiple conformations corresponding to multiple degrees of activation [38–43].

In the realm of drug discovery, the potential impact of X-ray structures of ligand-mediated GPCRs now can be evaluated with these β_2 AR structures. Using the high-resolution β_2 AR X-ray structure as a prototype for drug discovery with the structure of the protein of interest, it was very quickly shown that database mining with high-throughput docking alone could extract low-nanomolar compounds from large databases with high efficiency [44]. This demonstrated that “production-quality” results now could be obtained from X-ray structures of GPCRs. Additionally, the accuracy of predicted binding modes [44] was validated shortly thereafter with the publication of the X-ray structure of β_2 AR bound with the antagonist timolol [45,46]. Retrospective and prospective assessment of the use of ligand-mediated GPCR X-ray structures as templates for homology models for other GPCR targets has now become possible. Retrospectively, in a direct comparison of the use of two structures, Costanzi has shown [47] that the results of docking carazolol into a rhodopsin-based homology model of β_2 AR gave qualitatively poorer results than the direct use of the β_2 AR X-ray structure. Similarly, the predicted binding mode of epinephrine to another rhodopsin-based homology model of β_2 AR resulted in a different mode of interaction of the hydroxyl alkylamine moiety than that of its identical counterpart in carazolol [48]. Whether or not this difference is an artifact of the model or, e.g., due to the fact that epinephrine is an agonist, which may bind differently, is unknown. Prospectively, the use of a

ligand-mediated GPCR template, the β_2 AR X-ray structure, for predicting other class A GPCR structures has already begun [49,50]. For example, an opportunity to evaluate this approach has already appeared with the publication [51] of the X-ray complex of the A_{2A} adenosine receptor protein with the antagonist ZM241385. When comparing the ZM241385 binding to a β_2 AR-based homology model [49] of the A_{2A} adenosine receptor, the binding of ZM241385 in the X-ray structure is very different in both mode and location (see below). Similarly, the use of the β_2 AR X-ray structure for agonist drug discovery has already begun [52–54]. de Graaf and Rognan showed [52] that the use of the coordinates of the β_2 AR X-ray structure, when modified to a model calibrated to more closely represent a closed (active) form of the binding pocket expected for agonist binding, provides improved efficiency in database mining for agonists. Audet and Bouvier performed [55] docking studies with various β_2 AR ligands to explore hypotheses for differential activation of adenylyl cyclase vs. mitogen-activated protein kinase.

4.2. The β_2 -adrenergic receptor/timolol complex: the first iterative crystallization

A second high-resolution β_2 AR X-ray structure, now with the partial inverse agonist timolol as the ligand, has already been reported [45]. The approach of splicing T4L into the ICL3 region was repeated and the overall structure was very similar, with only small active-site conformational changes, which are consistent with expectations for the different ligand. Not surprisingly, the binding of timolol to β_2 AR is very similar to that of carazolol. The hydroxy alkylamine side-chain forms the same hydrogen-bonding patterns with Asp113 and Asn312. The ligand's hydrophobic portions sit in the same region as well. The side-chain rotamer conformation of Asn293 has however shifted towards the ligand to form a hydrogen bond with the morpholine oxygen atom of timolol. As the earlier β_2 AR X-ray structure with carazolol was used to dock a number of known ligands [44], including timolol, this timolol-bound β_2 AR X-ray structure allowed a quick assessment of the use of the X-ray structure for predicting binding modes. Encouragingly, the docked [44,46] (to the carazolol/ β_2 AR X-ray) result and this timolol/ β_2 AR X-ray structure showed good agreement.

Interestingly, because the crystal packing is different in the two structures, two cholesterol binding sites, which are not involved in crystal packing, are revealed in the latter structure. These binding sites may play a role in cholesterol-mediated thermal stabilization, allosteric modulation of ligand binding to the high-affinity agonist binding state, and receptor trafficking (see Ref. [45] and references therein).

4.3. The β_1 -adrenergic receptor/cyanopindolol complex: the second ligand-mediated GPCR to be crystallized

The X-ray structure of another ligand-mediated GPCR appeared [56] recently as well. The structure is that of the antagonist cyanopindolol bound to the turkey β_1 -adrenergic receptor. The close relationship of these proteins, i.e., β_1 AR vs. β_2 AR, belies the significance of this work. While the same underlying principles, e.g., stabilization of the protein complex, again played critical roles in the protocol, the actual methods used were very different. Specifically, through extensive analyses of the thermal stabilizing effects of various mutants and their combinations, a composite of six mutations was introduced to sufficiently stabilize the complex without the introduction of a companion (mAb or T4L) protein. (Excisions of residues in ICL3 and the C-terminus were also made.) This provided a striking validation of the underlying principles. Because β_1 AR and β_2 AR are so closely related, comparing their structures is particularly meaningful. The two structures are in fact

very similar, thereby providing striking reciprocal validation of the common underlying principles of both approaches, which could conceivably open the door to yet other approaches capitalizing on them. This agreement of the structures speaks directly to the possible concern of dramatic artifacts in the use of a companion protein in the above cited β_2 AR structures. The ligand-binding sites are very similar with expected differences due to different bound ligands and small variations in the binding-site residues. The amino acid differences close to the ligand are so few that the source of selectivity is not obvious. Thus, the hydroxy alkylamino side-chain of cyanopindolol is anchored by two hydrogen bonds each from Asp121 and Asn329 (see Figs. 1 and 2). The aromatic indole group of cyanopindolol overlaps with, e.g., the carazolol carbazole component. Asn310 interacts with the nitrogen atom of the cyano group, akin to the corresponding Asn293 interaction with the morpholine oxygen atom of timolol in the β_2 AR structure. Among the more notable differences found between the β_1 AR and β_2 AR structures are the residues in the “ionic-lock” region. While here too, the “ionic lock” observed in rhodopsin is not formed, there are differences with respect to β_2 AR. A short α -helix is formed in ICL2, thereby accommodating a hydrogen bond between Tyr149 on ICL2 and Asp138 of the “ionic lock” on H3 (see panel C of Fig. 3). This character of the ICL2 structure in this region is preserved in all four molecules of the unit cell of the X-ray structure of β_1 AR, even though they make different internal crystal contacts, whereas this is not found in the β_2 AR/carazolol structures. After considering related mutational data, the authors conclude that this is the physiological relevant structure. The β_1 AR protein does not have basal activity and, when bound with the antagonist cyanopindolol, lacks the “ionic lock” in common with the β_2 AR structures. This leads to the authors' conclusion that there is no evidence of the “ionic lock.” Alternatively (also see below), the Asp138-to-Tyr149 hydrogen bond may cause full antagonism, which would explain the inactivity of the cyanopindolol β_1 AR structure in contrast to the residual basal activity of the two β_2 AR complexes with inverse agonists.

4.4. The A_{2A} adenosine receptor: the third ligand-mediated GPCR to be crystallized moves away from the biogenic amines

All of the reported ligand-mediated GPCR X-ray structures described above are receptors for monoaminergic ligands. A recent publication [51] has now provided the X-ray structure of the A_{2A} adenosine receptor in complex with the high-affinity antagonist ZM241385. While still within the class A receptors, this more distal GPCR result confirms the ability of the T4L fusion protein approach to be extendable to other targets. The structure itself provides yet more information and new insights. The extracellular loop ECL2 resembles neither the extended β -sheet of rhodopsin nor does it include the α -helix structure of the adrenergic receptors (see panel B of Fig. 1). Rather, ECL2 adopts a random coil conformation that has three cysteine bridges to EC1 and one within EC2, resulting in an opening that could accommodate entry of small molecules into the active site. Additionally, a number of the transmembrane helices of the A_{2A} adenosine receptor are shifted significantly with respect to either rhodopsin or the adrenergic receptors. Probably as a consequence of the helical shifts and change in ECL2 architecture, the binding of the antagonist ZM241385 is very different from that of the adrenergic receptor ligands (see panels B and D of Figs. 1 and 2) in that it sits much closer to the extracellular side with little overlap of the corresponding ligands. This region is closer to where peptidic ligands are expected to bind to their corresponding receptors. The furan ring of ZM241385 sits deepest within the binding site, forming a hydrogen bond with Asn253 and hydrophobic interaction with His250 and Leu249. The central triazolotriazine unit of ZM241385 forms hydrogen bonds with

Asn253 and Glu169 and hydrophobic interactions with Ile274 and Phe168. The hydroxyphenyl ring sits furthest from the core and forms hydrophobic interactions with Leu267 and Met270. Trp246, the so-called “toggle-switch” residue, is held in the inactive conformation by the furan ring. These differences in both binding mode and location of the A_{2A} adenosine receptor ligand lead the authors to the reasonable projection that major selectivity differences among more distant GPCRs is not rooted in a subset of varying amino acids on a backdrop of a common/rigid backbone, but from a broad plasticity of the receptors allowing a reorientation and relocation of different ligands in their receptors. This suggests that there may be significant limitations on the direct use of X-ray structures as templates for homology models of more remotely related GPCRs (also see Ref. [30]). The practical consequences of this can already be exemplified from studies published using the new X-ray structures summarized herein. A homology model for the A_{2A} adenosine receptor with ZM241385 bound, based on the high-resolution carazolol/ β_2 AR X-ray structure, has already appeared [49]. In contrast to the A_{2A} adenosine receptor X-ray structure, the homology model finds ZM241385 bound in a similar site as carazolol in the high-resolution β_2 -AR X-ray structure. A similar discrepancy occurs with the use of a bovine-rhodopsin-based model [49].

With regard to the “toggle switch”, while the A_{2A} adenosine receptor X-ray structure finds the ligand further away from W6.48, the protein is still held in the inactive conformation, where His250 is recruited analogously to Phe290 in the β_2 AR structure (see panel E of Fig. 1). The “ionic lock” region is qualitatively similar in structure to that of the β_1 AR X-ray structure with an α -helix in ICL2 which provides Tyr112^{3,60} for interaction with Asp101^{3,49}. This demonstrates that these features can indeed be achieved in a T4L construct (see above). These authors therefore suggest that the absence of the ICL2 α -helix and, consequently, the absence of the Tyr112^{3,60}-to-Asp101^{3,49} interaction in the β_2 AR X-ray structures is correlated with their basal activity.

4.5. Return to opsin/rhodopsin: still breaking new ground

In spite of the fairly regular appearance of X-ray structures of rhodopsin, recent publications have now yielded the most direct elucidation of GPCR activation [57–61]. In May and June of 2008, two X-ray structures were published of the invertebrate squid rhodopsin which couples to G_q . The most distinguishing feature of these structures occurred in the intracellular region of H5 and H6 and the intervening loop ICL3 that has a 12-residue insertion compared with rhodopsin. In this region, these two helices are longer and rigid, extending well away from the core, and in one structure [58] form one side of a binding region for an occluded octylglucoside. These papers indicated that the surface around this extended region may be that needed to bind the G-protein. Shortly thereafter, in July and September, the two bovine opsin papers appeared. Both X-ray structures are believed to be in an active conformation. The more recent one is complexed with an eleven amino acid peptide, $G\alpha_{CT}$, derived from the C-terminal of the transducin $G\alpha_t$ protein [ILENLKDCGLF, $G\alpha_t$ (340–350K341L)] providing clear support for the active state. Building on an earlier approach [62], the authors selectively extracted bovine opsin from rod cell disc membranes. Among the salient features that distinguish these from the earlier rhodopsin structures are changes in the intracellular (IC) region. The α -helix of the intracellular side of H5 is elongated by 1.5–2.5 helical turns and is tilted inward toward the 7-TM core (see panel D of Fig. 3). The IC side of H6 is tilted outward by 6–7 Å as expected from earlier studies [63–65]. The combination of these two changes result in the alignment of H5 and H6, which protrude into the IC region (see panels A and B of Fig. 3). Residues of the highly conserved E(D)R135Y and

NPxxY306(x)_{5,6}F motifs play key roles in these changes (see panels C and D of Fig. 3). Serving as a latch, Glu247 of H6 decouples from Arg135 of H3, allowing H6 to move out and away from H3 and swing over to H5 so that Glu247 can form a salt bridge with Lys231 of H5, helping position H6 closer to H5. Tyr223 of H5 now interacts with Arg135 of H3, positioning H5 inward towards H3. Tyr306 of H7 is rotated into the helix core, thereby blocking the inward return of H6. Binding of the $G\alpha_{CT}$ peptide again involves Arg135 through the formation of a hydrogen bond to the backbone carbonyl oxygen atom of Cys347 of $G\alpha_{CT}$. $G\alpha_{CT}$ sits in a crevice formed by H5 and H6 on one side, providing mainly hydrophobic interactions, and H7 and H8, providing a hydrogen-bonding network (see panel B of Fig. 3). Relative to the earlier rhodopsin structures, the kink between H7 and H8 bends away from the core, which, together with the changes in H5 and H6, is required to accommodate $G\alpha_{CT}$ binding [59,60]. None of the ligand-mediated X-ray structures contains the full, native ICL3 loop, thereby confounding such detailed analysis in this region. Other regions of these two X-ray structures are also informative. Trp265 of the “toggle switch” shifts in its position relative to the conformation in the X-ray structures of the inactive state but does not undergo the expected change in rotamer form (see panel E of Fig. 1). In the $G\alpha_{CT}$ -free X-ray structure, the electron density of Lys296, which forms the covalent bond to retinal in rhodopsin, is poorly defined, whereas the electron density improves significantly when $G\alpha_{CT}$ is bound, indicating that the $G\alpha_{CT}$ interaction influences the “ligand-binding” region. As the authors suggest, this supports the notion of these two regions being coupled in the activation process. Also observed are two openings in the extracellular region, one between TM5 and TM6 and the other between TM1 and TM7, which the authors suggest may provide the route for retinal entry (in the 11-cis form) and exit (in the all-trans form), respectively. These features are clearly different, e.g., from those of the adrenergic structures described above, and are necessitated by the blockage of the entryway by EC2 observed in opsin/rhodopsin. Furthermore, these “openings” are a consequence of helix motions on the EC side of the protein which change the ligand-binding site. Moreover, in addition to advancing the understanding of GPCR activation, these structures now will provide valuable template information for developing homology models for agonist binding.

5. Conclusions

The pervasive role of GPCRs in signal transduction and their consequent predominance as therapeutic targets have long been evident. To better understand the structure/function relationships of GPCRs and to more effectively design drugs for these proteins, researchers have long sought GPCR detailed atomic structures, as revealed through X-ray crystallography. The structural determination in 2000 of the light-activated class A GPCR, rhodopsin in the inactive state, was followed by a 7-year hiatus before another (non-rhodopsin) GPCR X-ray structure was published in 2007. In slightly more than a year since that publication, a relative surge of X-ray structures of ligand-mediated GPCRs and related publications have appeared. The use of different approaches to determine these X-ray structures, with related underlying principles, already suggest that the *rate* of generation of yet other X-ray structures will continue to accelerate. The *need* for additional structures for drug design is clear, as demonstrated by the significant differences of the ligand-binding features observed for ligands in the β_1 AR and β_2 AR vs. the A_{2A} adenosine receptor X-ray structures. It is clear that for GPCRs that are less closely related to these, such as class B or class C GPCRs, the construction of accurate homology models will remain difficult. Nevertheless, with the advances in understanding provided by the present successes, the use of the underlying principles to more rapidly solve other structures is now much more

promising. Regarding the *value* of GPCR X-ray structures for use in drug discovery, the use of the β_2 AR X-ray has already allowed the demonstration that nanomolar inhibitors can quickly be obtained for the protein used. Thus, a major goal of GPCR structure determination has been validated. Encouraging results are already emerging for homology modeling. As for the understanding of the mechanism of activation at the atomic level, the opsin/rhodopsin GPCR is again leading the way, in elucidating the understanding of the requirements for full activation. Structures of the ligand-mediated β_1 AR, β_2 AR, and the A_{2A} adenosine GPCRs are providing significant advances in the understanding of the partially/fully inactive states, albeit more clarity is needed. At this point, some of the major GPCR X-ray structure milestones to look forward to, particularly for the advancement of drug design, include those of other classes and subclasses, those for ligands of other character (e.g., agonists, allosteric modulators, etc.), other protein states, and dimeric structures. To be sure, these pursuits will remain challenging and the results will continue to be replete with surprises. What has become clear in the past year is that the rate of structure determination and the advances in our understanding has now accelerated significantly.

References

- [1] Lundstrom KH, Chiu ML, editors. G protein-coupled receptors in drug discovery. CRC Press; 2006.
- [2] Overington JP, Al-Lazikani B, Hopkins AL. How many drug targets are there? *Nat Rev Drug Discov* 2006;5(12):993–6.
- [3] Parrill AL. Crystal structures of a second G protein-coupled receptor: triumphs and implications. *ChemMedChem* 2008;3:1021–3.
- [4] Weis WI, Kobilka BK. Structural insights into G-protein-coupled receptor activation. *Curr Opin Struct Biol* 2008;18:734–40.
- [5] Mustafi D, Palczewski K. Topology of class A G protein-coupled receptors: insights gained from crystal structures of rhodopsins, adrenergic and adenosine receptors. *Mol Pharmacol* 2009;75:1–12.
- [6] Okada T, Fujiyoshi Y, Silow M, Navarro J, Landau EM, Shichida Y. Functional role of internal water molecules in rhodopsin revealed by X-ray crystallography. *Proc Natl Acad Sci USA* 2002;99:5982–7.
- [7] Archer E, Maigret B, Escricuet C, Pradayro L, Fourmy D. Rhodopsin crystal: new template yielding realistic models of G-protein-coupled receptors? *Trends Pharmacol Sci* 2003;24(1):36–40.
- [8] Bissantz C, Bernard P, Hibert M, Rognan D. Protein-based virtual screening of chemical databases. II. Are homology models of G-protein coupled receptors suitable targets? *Proteins Struct Funct Genet* 2003;50:5–25.
- [9] Barton N, Blaney FE, Garland S, Tehan B, Wall I. Seven transmembrane G protein-coupled receptors: insights for drug design from structure and modeling. *Compr Med Chem II* 2007;669–701.
- [10] Unwin PNT, Henderson R. Molecular structure determination by electron microscopy of unstained crystalline specimens. *J Mol Biol* 1975;94:425–40.
- [11] Baldwin JM, Henderson R, Beckman E, Zemlin F. Images of purple membrane at 2.8 Å resolution obtained by cryo-electron microscopy. *J Mol Biol* 1988;202(3):585–91.
- [12] Unger VM, Schertler GFX. Low resolution structure of bovine rhodopsin determined by electron cryo-microscopy. *Biophys J* 1995;68:1776–86.
- [13] Pebay-Peyroula E, Rummel G, Rosenbusch JP, Landau EM. X-ray structure of bacteriorhodopsin at 2.5 Å from microcrystals grown in lipidic cubic phases. *Science* 1997;277:1676–81.
- [14] Luecke H, Schobert B, Richter H-T, Cartailler J-P, Lanyi JK. Structure of bacteriorhodopsin at 1.55 Å resolution. *J Mol Biol* 1999;291:899–911.
- [15] Röper D, Jacoby E, Krüger P, Engels M, Grötzinger J, Wollmer A, et al. Modeling of G-protein coupled receptors with bacteriorhodopsin as a template. A novel approach based on interaction energy differences. *J Recept Res* 1994;14:167–86.
- [16] Underwood DJ, Strader CD, Rivero R, Patchett AA, Greenlee W, Prendergast K. Structural model of antagonist and agonist binding to the angiotensin II, AT₁ subtype, G protein coupled receptor. *Chem Biol* 1994;1(4):211–21.
- [17] Gershengorn MC, Osman R. Minireview: insights into G protein-coupled receptor function using molecular models. *Endocrinology* 2001;142(1):2–10.
- [18] Klabunde T, Hessler G. Drug design strategies for targeting G-protein-coupled receptors. *ChemBioChem* 2002;3:928–44.
- [19] Becker OM, Shacham S, Marantz Y, Noiman S. Modeling the 3D structure of GPCRs: advances and application to drug discovery. *Curr Opin Drug Discov Dev* 2003;6(3):353–61.
- [20] Reggio PH. Computational methods in drug design: modeling G protein-coupled receptor monomers, dimers, and oligomers. *AAPS J* 2006;8(2):E322–36.
- [21] Mobarec JC, Filizola M. Advances in the development and application of computational methodologies for structural modeling of G-protein-coupled receptors. *Exp Opin Drug Discov* 2008;3(3):343–55.
- [22] Schertler GFX, Villa C, Henderson R. Projection structure of rhodopsin. *Nature* 1993;362:770–2.
- [23] Patry A, Desai PV, Avery MA. Homology modeling of G-protein-coupled receptors and implications in drug design. *Curr Med Chem* 2006;13(14):1667–91.
- [24] Xie X-Q, Chen J-Z, Billings EM. 3D structural model of the G-protein-coupled cannabinoid CB₂ receptor. *Proteins Struct Funct Genet* 2003;53(2):307–19.
- [25] Vaidehi N, Floriano WB, Trabanino R, Hall SE, Freddolino P, Choi EJ, et al. Prediction of structure and function of G protein-coupled receptors. *Proc Natl Acad Sci USA* 2002;99:12622–7.
- [26] Shacham S, Topf M, Avisar N, Glaser F, Marantz Y, Bar-Haim S, et al. Modeling the 3D structure of GPCRs from sequence. *Med Res Rev* 2001;21(5):472–83.
- [27] Kortagere S, Welsh WJ. Development and application of hybrid structure based method for efficient screening of ligands binding to G-protein coupled receptors. *J Comput Aided Mol Des* 2006;20(12):789–802.
- [28] Moro S, Defflorian F, Bacilieri M, Spalluto G. Ligand-based homology modeling as attractive tool to inspect GPCR structural plasticity. *Curr Pharm Des* 2006;12(17):2175–85.
- [29] Rasmussen SGF, Choi H-J, Rosenbaum DM, Kobilka TS, Thian FS, Edwards PC, et al. Crystal structure of the human β_2 adrenergic G-protein-coupled receptor. *Nature* 2007;450:383–8.
- [30] Cherezov V, Rosenbaum DM, Hanson MA, Rasmussen SGF, Thian FS, Kobilka TS, et al. High-resolution crystal structure of an engineered human β_2 -adrenergic G protein-coupled receptor. *Science* 2007;318:1258–65.
- [31] Rosenbaum DM, Cherezov V, Hanson MA, Rasmussen SGF, Thian FS, Kobilka TS, et al. GPCR engineering yields high-resolution structural insights into β_2 -adrenergic receptor function. *Science* 2007;318:1266–73.
- [32] Faham S, Boulting GL, Massey EA, Yohannan S, Yang D, Bowie JU. Crystallization of bacteriorhodopsin from bicelle formulations at room temperature. *Protein Sci* 2005;14:836–40.
- [33] Landau EM, Pebay-Peyroula E, Neutze R. Structural and mechanistic insight from high resolution structures of archaeal rhodopsins. *FEBS Lett* 2003;555:51–6.
- [34] Cherezov V, Peddi A, Muthusubramanian L, Zheng YF, Caffrey M. A robotic system for crystallizing membrane and soluble proteins in lipidic mesophases. *Acta Crystallogr* 2004;D60:1795–807.
- [35] Ballesteros JA, Weinstein H. Integrated methods for the construction of three-dimensional models and computational probing of structure–function relations in G protein-coupled receptors. *Methods Neurosci* 1995;25:366–428.
- [36] Ballesteros J, Kitanovic S, Guarnieri F, Davies P, Fromme BJ, Konvicka K, et al. Functional microdomains in G-protein-coupled receptors. The conserved arginine-cage motif in the gonadotropin-releasing hormone receptor. *J Biol Chem* 1998;273(17):10445–53.
- [37] Ballesteros JA, Jensen AD, Liapakis G, Rasmussen SGF, Shi L, Gether U, et al. Activation of the β_2 -adrenergic receptor involves disruption of an ionic lock between the cytoplasmic ends of transmembrane segments 3 and 6. *J Biol Chem* 2001;276(31):29171–7.
- [38] Barak LS, Ménard L, Ferguson SSG, Colapietro A-M, Caron MG. The conserved seven-transmembrane sequence NP(X)₂Y of the G-protein-coupled receptor superfamily regulates multiple properties of the β_2 -adrenergic receptor. *Biochemistry* 1995;34:15407–14.
- [39] Ghanouni P, Gryczynski Z, Steenhuis JJ, Lee TW, Farrensi DL, Lakowicz JR, et al. Functionally different agonists induce distinct conformations in the G protein coupling domain of the β_2 adrenergic receptor. *J Biol Chem* 2001;276:24433–6.
- [40] Swaminath G, Xiang Y, Lee TW, Steenhuis J, Parnot C, Kobilka BK. Sequential binding of agonists to the β_2 adrenoceptor. Kinetic evidence for intermediate conformational states. *J Biol Chem* 2004;279(11):686–91.
- [41] Swaminath G, Deupi X, Lee TW, Zhu W, Thian FS, Kobilka TS, et al. Probing the β_2 adrenoceptor binding site with catechol reveals differences in binding and activation by agonists and partial agonists. *J Biol Chem* 2005;280(23):22165–71.
- [42] Yao X, Parnot C, Deupi X, Ratnala V, Swaminath G, Farrens D, et al. Coupling ligand structure to specific conformational switches in the β_2 -adrenoceptor. *Nat Chem Biol* 2006;2(8):417–22.
- [43] Kobilka BK, Deupi X. Conformational complexity of G-protein-coupled receptors. *Trends Pharmacol Sci* 2007;28(8):397–406.
- [44] Topiol S, Sabio M. Use of the X-ray structure of the Beta2-adrenergic receptor for drug discovery. *Bioorg Med Chem Lett* 2008;18:1598–602.
- [45] Hanson MA, Cherezov V, Griffith MT, Roth CB, Jaakola V-P, Chien EYT, et al. A specific cholesterol binding site is established by the 2.8 Å structure of the human β_2 -adrenergic receptor. *Structure* 2008;16:897–905.
- [46] Sabio M, Jones K, Topiol S. Use of the X-ray Structure of the β_2 -adrenergic Receptor for Drug Discovery. Part 2: Identification of Active Compounds. *Bioorg Med Chem Lett* 2008;18:5391–5.
- [47] Costanzi S. On the applicability of GPCR homology models to computer-aided drug discovery: a comparison between *in silico* and crystal structures of the β_2 -adrenergic receptor. *J Med Chem* 2008;51:2907–14.
- [48] Freddolino PL, Kalani MYS, Vaidehi N, Floriano WB, Hall SE, Trabanino RJ, et al. Predicted 3D structure for the human β_2 adrenergic receptor and its binding site for agonists and antagonists. *PNAS* 2004;101(9):2736–41.
- [49] Yuzlenko O, Kieć-Kononowicz K. Molecular modeling of A1 and A2A adenosine receptors: comparison of rhodopsin- and β_2 -adrenergic-based homology models through the docking studies. *J Comp Chem* 2008;30:14–32.
- [50] Selent J, López L, Sanz F, Pastor M. Multi-receptor binding profile of clozapine and olanzapine: a structural study based on the new β_2 adrenergic receptor template. *ChemMedChem* 2008;3:1194–8.
- [51] Jaakola V-P, Griffith MT, Hanson MA, Cherezov V, Chien EYT, Lane JR, et al. The 2.6 Å crystal structure of a Human A2A adenosine receptor bound to an antagonist. *Science* 2008;322:1211–7.

- [52] de Graaf C, Rognan D. Selective structure-based virtual screening for full and partial agonists of the β_2 adrenergic receptor. *J Med Chem* 2008;51(16):4978–85 [Erratum 51(20):6620].
- [53] Baker JG, Proudman RGW, Hawley NC, Fischer PM, Hill SJ. Role of key transmembrane residues in agonist and antagonist actions at the two conformations of the human β_1 -adrenoceptor. *Mol Pharm* 2008;74(5):1246–60.
- [54] Lee T, Schwandner R, Swaminath G, Weiszmann J, Cardozo M, Greenberg J, et al. Identification and functional characterization of allosteric agonists for the G protein-coupled receptor FFA2. *Mol Pharm* 2008;74(6):1599–609.
- [55] Audet M, Bouvier M. Insights into signaling from the β_2 -adrenergic receptor structure. *Nat Chem Biol* 2008;4:397–403.
- [56] Serrano-Vega MJ, Magnani F, Shibata Y, Tate CG. Conformational thermostabilization of the β_1 -adrenergic receptor in a detergent-resistant form. *Proc Natl Acad Sci USA* 2008;105:877–82.
- [57] Shimamura T, Hiraki K, Takahashi N, Hori T, Ago H, Masuda K, et al. Crystal structure of squid rhodopsin with intracellularly extended cytoplasmic region. *J Biol Chem* 2008;283:17753–6.
- [58] Murakami M, Kouyama T. Crystal structure of squid rhodopsin. *Nature* 2008;453:363–8.
- [59] Park JH, Scheerer P, Hofmann KP, Choe H-W, Ernst OP. Crystal structure of the ligand-free G-protein-coupled receptor opsin. *Nature* 2008;454:183–8.
- [60] Scheerer P, Park JH, Hildebrand PW, Kim YJ, Krauss N, Choe H-W, et al. Crystal structure of opsin in its G-protein-interacting conformation. *Nature* 2008;455:497–503.
- [61] Schwartz TW, Hubbell WL. A moving story of receptors. *Nature* 2008;455:473–4.
- [62] Okada T, Takeda K, Kouyama T. Highly selective separation of rhodopsin from bovine rod outer segment membranes using combination of divalent cation and alkyl(thio)glucoside. *Photochem Photobiol* 1998;67(5):495–9.
- [63] Cohen GB, Oprian DD, Robinson PR. Mechanism of activation and inactivation of opsin: role of Glu¹¹³ and Lys²⁹⁶. *Biochemistry* 1992;31(50):12592–601.
- [64] Vogel R, Siebert F. Conformations of the active and inactive states of opsin. *J Biol Chem* 2001;276(42):38487–93.
- [65] Lamb TD, Pugh Jr EN. Dark adaptation and the retinoid cycle of vision. *Prog Retin Eye Res* 2004;23:307–80.
- [66] Palczewski K, Kumasaka T, Hori T, Behnke CA, Motoshima H, Fox BA, et al. Crystal structure of rhodopsin: a G protein-coupled receptor. *Science* 2000;289:739–45.
- [67] Teller DC, Okada T, Behnke CA, Palczewski K, Stenkamp RE. Advances in determination of a high-resolution three-dimensional structure of rhodopsin, a model of G-protein-coupled receptors (GPCRs). *Biochemistry* 2001;40:7761–72.
- [68] Li J, Edwards PC, Burghammer M, Villa C, Schertler GFX. Structure of bovine rhodopsin in a trigonal crystal form. *J Mol Biol* 2004;343:1409–38.
- [69] Okada T, Sugihara M, Bondar A-N, Elstner M, Entel P, Buss V. The retinal conformation and its environment in rhodopsin in light of a new 2.2 Å crystal structure. *J Mol Biol* 2004;342:571–83.
- [70] Nakamichi H, Okada T. Local peptide movement in the photoreaction intermediate of rhodopsin. *Proc Natl Acad Sci USA* 2006;103(34):12729–34.
- [71] Nakamichi H, Okada T. Crystallographic analysis of primary visual photochemistry. *Angew Chem Int Ed Engl* 2006;45:4270–3.
- [72] Salom D, Lodowski DT, Stenkamp RE, Trong IL, Golczak M, Jastrzebska B, et al. Crystal structure of a photoactivated deprotonated intermediate of rhodopsin. *Proc Natl Acad Sci USA* 2006;103(44):16123–8.
- [73] Standfuss J, Xie G, Edwards PC, Burghammer M, Oprian DD, Schertler GFX. Crystal structure of a thermally stable rhodopsin mutant. *J Mol Biol* 2007;372:1179–88.
- [74] Nakamichi H, Buss V, Okada T. Photoisomerization mechanism of rhodopsin and 9-*cis*-rhodopsin revealed by X-ray crystallography. *Biophys J Biophys Lett* 2007;92:L106–8.
- [75] Stenkamp RE. Alternative models for two crystal structures of bovine rhodopsin. *Acta Crystallogr Sect D* 2008;64:902–4.
- [76] Schrödinger LLC. Maestro v8.5. Portland, Oregon, US; 2008.
- [77] Chemical Computing Group Inc. MOE v2007.0902. 1010 Montreal, Quebec, Canada; 2007.